

# Parameter-Efficient Fine-Tuning for Medical Image Analysis: The Missed Opportunity

Raman Dutt  
The University of Edinburgh  
Edinburgh, UK  
raman.dutt@ed.ac.uk

Linus Ericsson  
The University of Edinburgh  
Edinburgh, UK  
linus.ericsson@ed.ac.uk

Pedro Sanchez  
The University of Edinburgh  
Edinburgh, UK  
pedro.sanchez@ed.ac.uk

Sotirios A. Tsaftaris  
The University of Edinburgh  
Edinburgh, UK  
S.Tsaftaris@ed.ac.uk

Timothy Hospedales  
The University of Edinburgh  
Edinburgh, UK  
t.hospedales@ed.ac.uk

## Abstract

We present a comprehensive evaluation of Parameter-Efficient Fine-Tuning (PEFT) techniques for diverse medical image analysis tasks. PEFT is increasingly exploited as a valuable approach for knowledge transfer from pre-trained models in natural language processing, vision, speech, and cross-modal tasks, such as vision-language and text-to-image generation. However, its application in medical image analysis remains relatively unexplored. As foundation models are increasingly exploited in the medical domain, it is crucial to investigate and comparatively assess various strategies for knowledge transfer that can bolster a range of downstream tasks. Our study, the first of its kind (to the best of our knowledge), evaluates 16 distinct PEFT methodologies proposed for convolutional and transformer-based networks, focusing on image classification and text-to-image generation tasks across six medical datasets ranging in size, modality, and complexity. Through a battery of more than 600 controlled experiments, we demonstrate performance gains of up to 22% under certain scenarios and demonstrate the efficacy of PEFT for medical text-to-image generation. Further, we reveal the instances where PEFT methods particularly dominate over conventional fine-tuning approaches by studying their relationship with downstream data volume.

## 1. Introduction

Medical imaging technologies are revolutionizing modern medicine in various domains, covering both clinical diagnosis and biomedical research [32]. AI models have demonstrated diagnostic capabilities on par with human experts across a range of imaging modalities, including radiology [20, 50], dermatology [21], and ophthalmology [15, 75], among others. Such AI methods offer the potential to enhance healthcare access and overall health outcomes for society [77], making them

highly significant. However, a critical obstacle in achieving this vision is the need for large training datasets essential for mainstream end-to-end supervised deep learning from scratch. This challenge continues to grow as state-of-the-art deep architectures [19] become increasingly large and consequently more data-hungry over time. Acquiring the necessary volume of data is typically unattainable at the required scale due to privacy restrictions and the long-tailed nature of medical conditions of interest and prohibitively expensive to annotate [70].

To tackle the data bottleneck, an expanding body of medical AI research [3, 4, 36] has adopted the *pre-train fine-tune* or *transfer learning* approach, where models undergo training in two stages: Pre-training is conducted on either out-of-domain non-medical images or unlabeled medical images, which are easier to acquire, allowing this stage to scale to larger datasets. Fine-tuning is then performed on in-domain medical images for the specific task. The assumption is that parameters are mostly set during pre-training and only require minimal fine-tuning for the target task. This approach has become increasingly important since the emergence of ‘foundation models’ [8] — powerful off-the-shelf pre-trained models — due to their use of large architectures, extensive pre-training datasets, and massive training computations. Several recent evaluations have used larger external datasets in this manner to significantly enhance performance on medical tasks of interest [3, 4, 36].

Within the transfer learning paradigm and leveraging the significant industrial efforts in foundation model development [8, 11], the remaining challenge lies in the fine-tuning process. The central issue is balancing the adaptation of the initial model to sufficiently specialize it for the medical task while avoiding overfitting to the training set, which would result in poor generalization to the testing set. This balance has been explored through various fine-tuning algorithms, such as regularized fine-tuning [25, 74]. However, parameter-efficient fine-tuning (PEFT) has recently gained traction [29, 34, 58, 73],

initially within the NLP community and subsequently in computer vision. The concept involves either carefully selecting a subset of parameters to fine-tune while keeping the rest frozen or introducing a small number of new parameters during the fine-tuning step and freezing all transferred parameters. While numerous PEFT architectures have emerged in NLP and vision literature, a comprehensive empirical evaluation comparing their effectiveness on a common benchmark is lacking in medical image analysis. Moreover, we observe that PEFT architectures are not widely adopted in medical vision tasks, despite the data-efficiency needs of the medical domain.

In this paper, we present an evaluation of state-of-the-art PEFT methods using medical image analysis benchmark tasks. We compare 16 state-of-the-art PEFT techniques across six medical datasets, encompassing both CNN and transformer architectures, discriminative diagnosis tasks, and a novel –first-of-a-kind demonstration of PEFT’s effectiveness– in a generative medical image synthesis task. We experiment with architectures that match the size of recent foundation models introduced for computer vision and medical image analysis [11, 42]. In addition, we investigate aspects such as the trade-off between PEFT effectiveness and data volume for the task at hand and the balance between parameter count and efficacy. Our extensive experiments offer the community of medical image analysis and medical vision valuable insights into which PEFT methods are best suited for their task and, more broadly, establish the first comprehensive comparison benchmark for PEFT in medical vision.

Our contributions can be summarised by the following questions and their answers:

**Q1:** *How effective is PEFT for low data scenarios?* **A1:** Given a large pre-trained model, benefits from PEFT increase as data volume decreases and model size increases (Sec. 4.1).

**Q2:** *Can PEFT improve transfer to discriminative medical tasks?* **A2:** Yes, three methods achieve consistent gains compared to full fine-tuning, two of which also significantly reduce the computational cost of tuning (Sec. 4.2).

**Q3:** *Can PEFT improve costly text-to-image generation?* **A3:** PEFT methods are less reliable in this setting but can still offer performance gains, with moderate reductions to computational cost (Sec. 4.3).

## 2. Related Work

### 2.1. Adapters

**Additive Methods.** Adapters are new modules added among the layers of a pre-trained network to reconfigure a given pre-trained model for a downstream task. The idea was originally introduced for learning representations that could aid in the analysis of multiple, diverse domains. [57, 58]. Li *et al.* [45] introduced Task-Specific Adapters (TSA) for learning multiple domains but with limited examples (cross-domain few-shot learning). Hounsby *et al.* [33] extended [57] for natural language processing by applying adapters to transformers. Hu *et*

al. [34] build upon [1] and introduce low-rank matrices into the self-attention layer of transformer-based models. This approach, termed *LoRA*, introduces no additional inference latency, as seen in [33], and has demonstrated superior performance over traditional model fine-tuning across diverse datasets and tasks. Lian *et al.* [47] propose a different parameter-efficient fine-tuning approach through Scaling and Shifting the Features (SSF) extracted by a pre-trained model. The difference in upstream and downstream data distribution poses a challenge to adapting pre-trained models to downstream datasets. SSF introduces parameters, after each network operation, that modulate (scale and shift) the extracted features of the downstream dataset such that they fall in a discriminative space. Chen *et al.* [13] introduced a novel PEFT approach designed for vision transformers for image and video recognition (*AdaptFormer*) and demonstrated that adding only 2% extra parameters to a vision transformer can outperform fully-finetuned networks on multiple benchmarks.

**Selective Methods.** This line of approach does not insert any new modules but finetunes a subset of the original pre-trained model. BitFit [7] proposes finetuning only the bias terms in a transformer-based model. In addition to being parameter-efficient, BitFit also alleviates catastrophic forgetting and matches full fine-tuning performance. Cai *et al.* [10] have drawn a similar parallel by fine-tuning only the bias terms in CNNs for on-device learning. Similarly, Frankle *et al.* [24] reveal the expressivity of parameters in the batch normalization layers, particularly, in shifting and rescaling random features. The SSF approach [47] described earlier, was developed on this understanding. Similar properties have also been revealed in Vision transformers [19]. Touvron *et al.* [66] show that fine-tuning only attention layers in vanilla ViTs is an effective strategy. Basu *et al.* [6] demonstrated that fine-tuning the parameters of normalization layers is very effective for few-shot classification.

**Prompt Tuning.** The concept of appending prompts to large language models has enabled powerful zero-shot and few-shot performance [9, 63]. Prompt tuning [43] introduced the idea of appending the input in language models with a trainable tensor, termed *soft prompt*. Jia *et al.* [37] extended this concept for vision transformers by proposing two schemes, *VPT-Deep* and *VPT-Shallow*. Similar to *VPT-Deep*, Li *et al.* [46] advocated the idea of appending trainable parameters in all hidden layers. Qin *et al.* [55] proposed adopting an autoencoder for decompressing the soft prompts to improve the convergence in [43]. A summary of different PEFT methods along with their categorization is given in Table 1.

### 2.2. PEFT for Text-to-Image Generation

Diffusion models [31] have led to state-of-the-art results in a variety of tasks such as text-to-image generation [5, 60, 62], image synthesis [18], density estimation [41] and many others. Recently, PEFT methods for text-to-image diffusion models have been proposed. Xie *et al.* [73] proposed *DiffFit*, for diffusion models based on transformers [54]. They found that

PEFT Method	Paper	Summary	CNNs	ViTs	PEFT Type
Task-Specific Adapters (TSA)	Li <i>et al.</i> [45]	Cross-domain few-shot learning by inserting learnable modules.	✓	✗	Additive
BatchNorm Tuning	Frankle <i>et al.</i> [24]	Training only BatchNorm layers (even with random initialization) leads to high performance in CNNs.	✓	✗	Selective
Bias Tuning	Cai <i>et al.</i> [10]	Propose TinyTL framework that learns only bias modules for parameter-efficient on-device learning.	✓	✗	Selective
Scale-Shift Features (SSF)	Lian <i>et al.</i> [47]	Adapt a pre-trained model to downstream datasets by introducing parameters that modulate the extracted features.	✓	✓	Additive
Attention Tuning	Touvron <i>et al.</i> [66]	Fine-tuning attention layers is sufficient to adapt ViTs to different classification tasks.	✗	✓	Selective
LayerNorm Tuning	Basu <i>et al.</i> [6]	Fine-tuning LayerNorm parameters is a strong baseline for few-shot adaptation.	✗	✓	Selective
BitFit	Zaken <i>et al.</i> [7]	Fine-tuning the bias terms in a transformer is competitive or better than full-fine-tuning.	✗	✓	Selective
LoRA	Hu <i>et al.</i> [34]	Training injected rank decomposition matrices in transformers is on-par or better than full-fine-tuning.	✗	✓	Additive
AdaptFormer	Chen <i>et al.</i> [13]	Adding lightweight modules increases a ViT’s transferability for different image and video tasks.	✗	✓	Additive
SV-Diff	Han <i>et al.</i> [28]	Fine-tuning singular values of weight matrices is a parameter-efficient adapter for text-to-image generation models.	U-Net and Text-Encoder in SD		Additive

Table 1. Summary of the Parameter-Efficient Fine-Tuning (PEFT) methods included in this evaluation, highlighting the specific model type they are designed for and their respective categories.

fine-tuning the bias terms is a strong baseline for downstream fine-tuning and further introduced learnable scaling factors at specific positions of the model for efficient adaptation. Moon *et al.* [51] identified fine-tuning the attention modules as another effective strategy and introduced an adapter that improves image-generation quality. Xiang *et al.* [72] presented the procedure for parameter-efficient fine-tuning in diffusion models by studying the design space of adapters in terms of position and function form. Han *et al.* [28] propose a new method, termed “SV-Diff”, for efficient personalization of text-to-image diffusion models. They designed a compact parameter space by fine-tuning singular values of weight matrices. This method is more parameter-efficient than existing approaches such as LoRA [34].

### 2.3. PEFT for Medical Image Analysis

There has been limited adoption of PEFT techniques within medical image analysis. Fischer *et al.* [23] modify a vanilla U-Net [61] with class-dependent learnable prompt tokens for semantic segmentation. Their approach almost matches the performance of a fully finetuned model on two medical datasets. Rodríguez *et al.* [64] study adapters designed for dense prediction tasks to improve medical image segmentation. Experiments with the recently proposed Segment Anything Model (SAM) [42] have revealed its inefficacy in the medical image analysis domain [17]. To overcome this, Wu *et al.* [71] combine the SAM model with adapters [33] and outperform existing state-of-the-art methods on several downstream medical segmentation tasks. Similarly, Zhang *et al.* [76] combined SAM with LoRA. In this work, we perform the first wide benchmarking study that applies PEFT techniques to diverse tasks in the medical image analysis domain, using state-of-the-art architectures.

## 3. Background

### 3.1. Problem Definition

The general problem definition for fine-tuning can be formalized as follows. Let  $f$  be a pre-trained model parameterized by  $\theta$ ,  $\ell$  be a loss function we wish to minimize and  $\mathcal{D} = \{(x_i, y_i)\}_i^N$  be the downstream dataset of interest, consisting of inputs  $x_i$  and their targets  $y_i$ . Starting from the initialization  $\theta = \theta_0$ , where  $\theta_0$  are the weights from pre-training, our objective is then to optimize by gradient descent the total loss

$$L = \frac{1}{N} \sum_{i=1}^N \ell(f(x_i; \theta), y_i). \quad (1)$$

Due to resource constraints, full fine-tuning like this is not always possible. It can also be suboptimal to tune the entirety of network weights, as many layers may have learned generally applicable features. Parameter-Efficient Fine-Tuning provides options in these cases, which fall into two broad families. **Selective** methods rely on optimising only a subset of model parameters,  $\phi \in \theta$ . This could be a subset of the layers or a specific type of parameter like batch norm. **Additive** methods instead introduce new parameters such that the full set becomes  $\theta' = \{\theta, \phi\}$  where  $\phi$  can be as simple as a new classifier layer or carefully designed adapters. For both families of methods, the update rule becomes

$$\phi = \phi - \eta \nabla_{\phi} L, \quad (2)$$

where  $\eta$  is the learning rate.

### 3.2. PEFT Methods For Comparison

In this section, we formally define the different fine-tuning protocols used in the analysis. We begin with a downstream

dataset  $D$  and a feature extractor  $f_\theta$  (pre-trained CNN (ResNet50) or a ViT (Base/Large/Huge)) expected to produce generalizable representations for diverse tasks. First, we freeze all the weights of this feature extractor and enable either an existing subset or a newly added parameter set according to the fine-tuning protocol.

In selective tuning methods, we permit specific parameters to be trainable based on the selected algorithm. For instance, for protocols like BatchNorm and Bias Tuning, the parameters of the ‘BatchNorm2d’ layers or the ‘bias’ terms are respectively made trainable. The training protocols for other selective methods are given in Appendix (Sec 6.3).

In **TSA**, our objective is to learn task-specific weights  $\phi$  to obtain the task-adapted classifier  $f_{(\theta,\phi)}$ . Next, we minimize the cross-entropy loss  $L$  over the samples in the downstream dataset  $D$  w.r.t the task-specific weights  $\phi$ . Li *et al.* [45] recommend the parallel adapter configuration. The output of the  $l$ -th layer of the feature extractor  $f_\theta$  can be combined with the task-specific adapters  $r_\phi$  for an input tensor  $h \in \mathbb{R}^{W \times H \times C}$  in a parallel configuration using Equation 3,

$$f_{(\theta,\phi)}(h) = r_\phi(h) + f_{\theta_l}(h). \quad (3)$$

In the **SSF** method, feature modulation is achieved by introducing scale ( $\gamma$ ) and shift ( $\beta$ ) parameters following each operation in the model. The previous operation’s output is multiplied by the scale parameter through a dot product and combined with the shift factor. Therefore, for a given input  $x$ , the output  $y$  is calculated using the formula  $y = \gamma \cdot x + \beta$ .

An **AdaptFormer** module (*AdaptMLP*) consists of two branches wherein the first branch is identical to the MLP block of a vanilla transformer while the second branch consists of a down-projection ( $W_{down}$ ), a ReLU layer, an up-projection ( $W_{up}$ ), and a scaling factor ( $s$ ). The adapted features ( $x_{adap}$ ), obtained using Equation 4, are combined with the original features entering the *AdaptMLP* block ( $x_{orig}$ ) through a residual connection, as defined in Equation 5.

$$x_{adap} = \text{ReLU}(\text{LN}(x_{orig}) \cdot W_{down}) \cdot W_{up} \quad (4)$$

$$x_{final} = \text{MLP}(\text{LN}(x_{orig})) + s \cdot x_{adap} + x_{orig} \quad (5)$$

**LoRA** is based on the concept that, during adaptation, weight updates exhibit low intrinsic rank. Consequently, when a pre-trained weight matrix  $W_0$  is updated, the change ( $\Delta W$ ) is characterized by a low-rank decomposition operation with rank  $r$ , as shown in Eqn. 6 where  $B \in \mathbb{R}^{d \times r}$  and  $A \in \mathbb{R}^{r \times k}$ ,

$$W_0 + \Delta W = W_0 + BA. \quad (6)$$

**SV-Diff** performs Singular Value Decomposition (SVD) of the weight matrices of a pre-trained diffusion model (Equation 7) and optimizes the spectral shift ( $\delta$ ), defined as the difference between singular values and of the updated and original weight

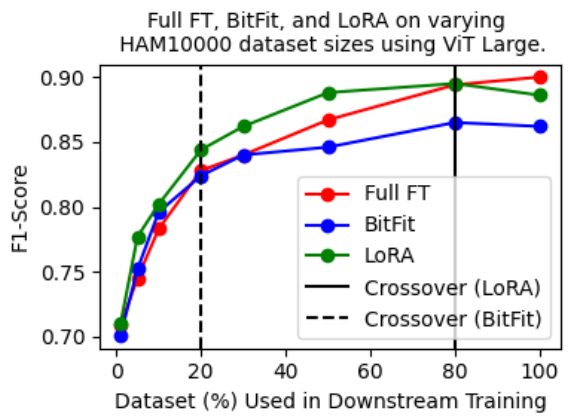
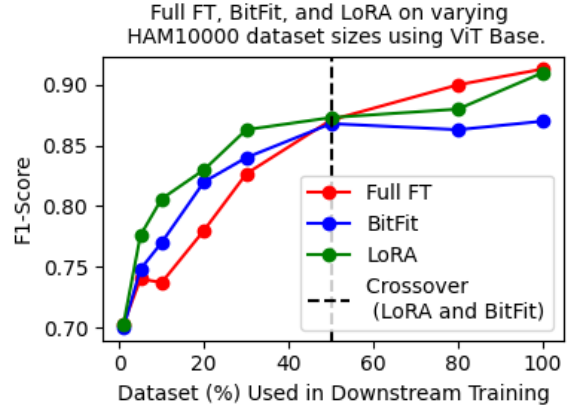


Figure 1. Plots showing the performance comparison for Full Fine-tuning, BitFit and LoRA with varying downstream dataset size for ViT-Base and ViT-Large models.

matrix. The update rule is defined in Eqn. 8,

$$W = U\Sigma V^\top \quad \text{with} \quad \Sigma = \text{diag}(\sigma), \quad (7)$$

$$W_\delta = U\Sigma_\delta V^\top \quad \text{with} \quad \Sigma_\delta = \text{diag}(\text{ReLU}(\sigma + \delta)). \quad (8)$$

## 4. Experiments

### 4.1. How Effective is PEFT For Low Data Scenarios?

**Setup.** In order to investigate the effectiveness of various fine-tuning approaches in relation to the downstream data volume, we utilized the HAM10000 dataset [67] and employed three distinct fine-tuning methods, namely Full Fine-tuning, BitFit, and LoRA, in combination with two different encoders, ViT Base and ViT Large. The performance of each method was evaluated by measuring the F1-Score at various dataset sizes, commencing with the entire sample size of 7,511 images (100%) and progressively reducing it to a minimum of 75 images (1%). To account for potential variability in the results, we report the average performance across three random seeds.

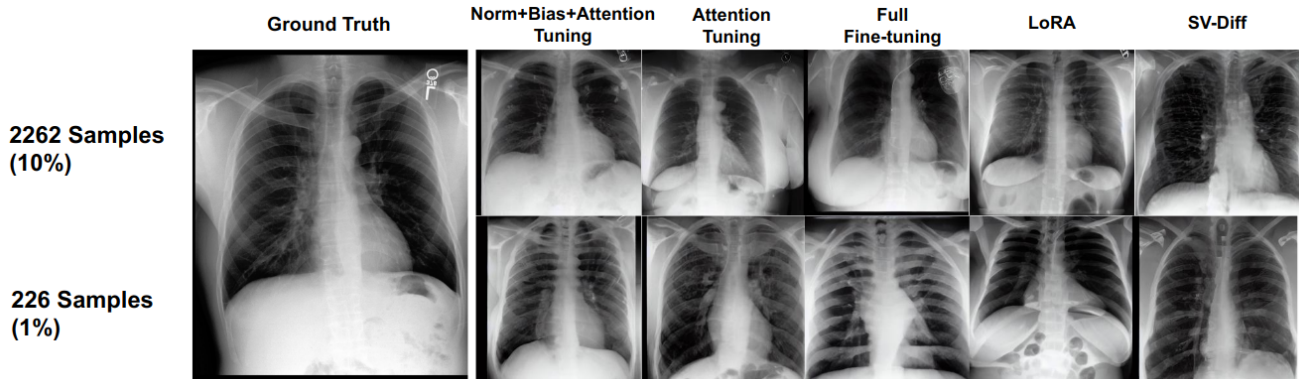


Figure 2. Figure showing text-to-image generation examples with the ground truth in the ascending average rank order (best five) for two data regimes. The input prompt for the generated samples is: “No acute cardiopulmonary process.”

**Results.** The results are shown in Figure 1. Starting with ViT Base on the left, we find that when using 100% of available downstream data, full fine-tuning is optimal, closely followed by LoRA. As the availability decreases, however, the benefits from PEFT approaches increase. The crossover is at 50%, when all approaches are approximately equal. For smaller data sizes, both PEFT approaches consistently outperform full FT, with LoRA providing gains of up to 6% over the baseline. For ViT Large, the trend is similar, but the crossover now differs between the PEFT approaches. LoRA overtakes the baseline as early as 80% while BitFit is only better at data volumes below 20%. Our take-home message here is that when data is scarce, coupled with a large upstream model, it becomes especially important to consider parameter-efficient tuning.

#### 4.2. Can PEFT Improve Transfer to Discriminative Medical Tasks?

**Setup.** In our discriminative experiments, we use five diverse datasets widely recognized in the medical image analysis community for image classification tasks, BreastUS [2], HAM10000 [67], Fitzpatrick17K [26,27], Standardized Multi-Channel Dataset for Glaucoma (SMDG) [?, ?], and RSNA Pneumonia Detection Dataset [52]. The experiments employ ResNet50 [30] and ViT (Base/Large/Huge) [19] as encoders. All CNN experiments employed ResNet50 pre-trained on ImageNet [16] while all ViT variants were pre-trained on ImageNet-21k [59]. Hyper-Parameter Optimization (HPO) was utilized to determine the optimal set of hyperparameters for each experiment. To ensure the timely completion of our search, the ASHA hyperparameter optimization algorithm [44] was adopted. For each dataset, various fine-tuning methods were applied using the hyperparameters obtained from the search, and performance was compared using a separate test set. During training, early stopping was implemented, halting the training process if the performance on the validation set did not improve for a predefined number of epochs.

**Results.** We present the results for ResNet-50 in Table 2. Given its convolutional architecture, ResNet-50 is compatible with certain PEFT methods but not others. Overall, full fine-tuning tends to outperform basic linear probing. Observations from the BreastUS and SMDG datasets indicate that most PEFT methods enhance performance beyond the full FT baseline. The SSF method, despite only tuning 60K parameters (0.25%), improves performance by up to 22%. While gains on HAM10000, FitzPatrick and Pneumonia are more modest, the previous section has discussed how these results could potentially vary with changes in data volume and model size. Overall, SSF emerges as the top-performing method based on average F1 score and ranking. Full fine-tuning and TSA present a close tie with the latter emerging on top. BatchNorm and bias tuning perform better than linear probing which turns out to be the worst strategy. Overall, the greatest gains are observed in the smallest dataset (BreastUS), however, the performance gap between full fine-tuning and PEFT methods minimizes with an increase in dataset size. For **Transformer** models in Tab. 3, the situation is similar. The biggest gains over full FT are on BreastUS and SMDG, while linear probing underperforms here as well. The top PEFT method is LoRA, for both average F1 score and rank, across all five datasets. AdaptFormer does not perform well and even falls behind linear probing for ViT Large. This can be attributed to the fact that this method was mainly designed for video recognition tasks. We also see that the benefits of PEFT increase slightly as the model size increases, with a 4% improvement for ViT Base going to 6% for ViT Huge. This is an interesting finding, and agrees with Sec. 4.1, as the proportion of parameters tuned actually decreases for the larger models.

Figure 3 illustrates the trade-off between each method’s performance and parameter count. This comparison is crucial as different applications may prioritize either superior performance or computational efficiency. For the results produced by the ResNet50 (shown on the left), each PEFT method lies on the Pareto frontier, indicating that a specific method could be

Method \ Dataset	Full FT (23.5M)	Linear Probing (3.8-7.2K)	TSA (10.6M)	BN Tuning (59.1K)	Bias Tuning (32.7K)	SSF (60.6K)
BreastUS (584)	0.72±1.1	0.61±1.3	0.90±0.8	0.92±0.9	0.89±1.2	<b>0.94±0.7</b>
FitzPatrick (5809)	<b>0.71±0.4</b>	0.66±0.8	0.69±1.4	0.67±1.1	0.64±1.3	<b>0.71±0.7</b>
HAM10000 (7511)	0.87±1.2	0.82±0.6	0.86±1.0	0.84±0.6	0.70±1.0	<b>0.89±0.9</b>
SMDG (9852)	0.75±0.9	0.69±1.0	<b>0.85±0.7</b>	0.83±1.4	0.73±0.6	0.84±0.9
Pneumonia (20412)	0.86±1.4	0.80±0.4	0.86±1.1	0.84±1.5	0.85±1.9	<b>0.87±1.2</b>
Average F1 Score	0.77	0.72	0.83	0.82	0.76	<b>0.85</b>
Average Rank	2.8	5.2	2.2	3.2	4.6	<b>1.2</b>

Table 2. Comparing different fine-tuning methods for ImageNet pre-trained ResNet50. Dataset size and parameter count are indicated in brackets. The best result for each dataset is highlighted, and the average rank for each fine-tuning method is shown at the end.

selected based on the prioritization of either performance or cost. Remarkably, the SSF method stands out by delivering high performance at a significantly reduced cost. In the case of the ViT-B model, LoRA emerges as the prominent choice, outpacing SSF while maintaining a similar computational expense.

To answer our question *can PEFT Improve Transfer to Discriminative Medical Tasks?* Yes, TSA, SSF and LoRA provide consistent improvements over full fine-tuning, and there is room to prefer less resource-intensive methods if necessary, requiring as little as 0.25% of parameters.

### 4.3. Can PEFT Improve Costly Text-to-Image Generation?

**Setup.** We use the MIMIC-CXR dataset (version 2.0.0) [38]. Following the recommendations in [12], we begin with fine-tuning the U-Net component (keeping text-encoder and VAE frozen) of the stable diffusion pipeline for different sizes of the downstream dataset (2262 and 226 samples, representing 10% and 1% of the original MIMIC-CXR dataset). We retained only those studies where the associated text reports had a character length between 7 and 77 tokens. Finally, we created a separate training set (subgroups P10 - P18) and a test set (subgroup P19). For analysis, we compare the full-finetuning of U-Net with 7 different PEFT methods and report the FID Score over 1000 test images averaged across three random seeds.

**Results.** Our results for this section can be found in (Table 4). Example images generated using different fine-tuning methods for the two scenarios are shown in Figure 2. For both data volumes, only a subset of PEFT methods yields performance enhancements over full fine-tuning. Simply fine-tuning attention layers turns out to be an effective strategy which can be further improved by simultaneous fine-tuning of attention, bias, and normalization layers (*bias+norm+attention*). This combination also outperforms full fine-tuning in both data regimes. Interestingly, both these methods require more computational resources than other PEFT methods but fine-tune merely 31% of parameters relative to the full FT. Consequently,

while current PEFT methods may not be as dependable for medical text-to-image generation as they are for classification tasks, they possess the potential to enhance performance and simultaneously decrease computational expenditure.

## 5. Conclusion

In this work, we have performed the first parameter-efficient fine-tuning evaluation for the medical image analysis domain. It has covered a diverse set of approaches and datasets and includes both discriminative and generative tasks. Our findings are (i) PEFT methods become more dominant with decreasing dataset size and increasing model size as full fine-tuning presents a risk of overfitting in this scenario; (ii) for discriminative tasks, the benefits from PEFT are especially prominent for low to medium-scale datasets, which are particularly common in the medical domain. Moreover, PEFT greatly reduces the computational and memory requirements, thereby making the application and adoption of large models much more practical in clinical settings; (iii) for text-to-image generation, the PEFT methods are less reliably effective, suggesting more work is needed in this area. However, generation quality can still be improved with a third of the parameters of full fine-tuning. As a recommendation, SSF and LoRA could be employed while adapting large convolution and transformer-based networks to medical tasks, respectively. Overall, PEFT methods should be an integral part of a medical AI practitioner’s toolbox.

## References

- [1] Armen Aghajanyan, Luke Zettlemoyer, and Sonal Gupta. Intrinsic dimensionality explains the effectiveness of language model fine-tuning. *arXiv preprint arXiv:2012.13255*, 2020. 2
- [2] Walid Al-Dhabyani, Mohammed Gomaa, Hussien Khaled, and Aly Fahmy. Dataset of breast ultrasound images. *Data in brief*, 28:104863, 2020. 5
- [3] Shekoofeh Azizi, Laura Culp, Jan Freyberg, Basil Mustafa, Sebastien Baur, Simon Kornblith, Ting Chen, Patricia MacWilliams, S. Sara Mahdavi, Ellery Wulczyn, Boris Babenko, Megan Wilson,

Encoder	Method	Full FT	Linear Probing	Attention Tuning	BitFit	LoRA	SSF	Adaptformer	LayerNorm Tuning
	Dataset								
ViT Base	BreastUS (584)	0.82±1.2	0.79±0.7	0.93±1.4	<b>0.97±1.3</b>	0.94±0.6	0.95±0.9	0.95±0.7	0.88±1.1
	FitzPatrick (5,809)	0.80±1.3	0.74±0.6	0.76±1.3	0.71±1.6	<b>0.82±1.4</b>	0.77±0.7	0.72±1.1	0.73±1.2
	HAM10000 (7,511)	<b>0.91±1.4</b>	0.72±0.5	0.86±1.2	0.87±1.8	<b>0.91±1.3</b>	0.88±0.8	0.76±1.2	0.85±1.3
	SMDG (9,852)	0.80±1.6	0.60±0.6	0.84±1.8	0.66±1.4	<b>0.86±1.5</b>	0.85±0.9	0.60±1.3	0.80±1.4
	Pneumonia (20,412)	0.87±1.7	0.86±0.4	0.85±1.1	0.87±1.2	0.86±0.8	<b>0.88±1.0</b>	0.83±0.9	0.87±1.7
	<b>Average F1 Score</b>	0.84	0.74	0.85	0.82	<b>0.88</b>	0.87	0.77	0.83
ViT Large	BreastUS (584)	0.84±1.8	0.73±0.7	0.86±1.3	<b>0.95±1.4</b>	0.93±1.3	0.92±1.8	<b>0.95±1.1</b>	0.88±1.4
	FitzPatrick (5,809)	<b>0.82±1.4</b>	0.74±0.5	0.77±1.2	0.74±1.5	<b>0.82±1.9</b>	0.80±1.3	0.72±1.2	0.78±1.3
	HAM10000 (7,511)	<b>0.90±1.6</b>	0.82±0.8	0.88±1.4	0.86±1.1	0.89±1.5	0.88±1.7	0.74±1.0	0.87±1.7
	SMDG (9,852)	0.81±1.5	0.77±0.6	0.84±1.5	0.83±1.9	0.83±1.2	<b>0.87±1.2</b>	0.63±1.3	0.85±1.5
	Pneumonia (20,412)	0.80±1.8	0.78±0.9	0.81±1.5	0.80±1.4	<b>0.82±1.1</b>	0.80±1.0	0.78±1.4	0.80±1.6
	<b>Average F1 Score</b>	0.83	0.77	0.83	0.84	<b>0.86</b>	0.85	0.76	0.84
ViT Huge	BreastUS (584)	0.92±1.8	0.67±0.9	0.89±1.5	<b>0.96±1.2</b>	0.86±1.8	<b>0.96±1.1</b>	0.93±1.0	0.92±1.4
	FitzPatrick (5,809)	0.69±1.3	0.72±0.6	0.70±1.3	0.72±1.2	<b>0.78±1.5</b>	0.73±1.1	0.72±1.4	0.72±0.8
	HAM10000 (7,511)	0.74±1.7	0.74±0.7	0.77±1.5	0.71±1.4	0.87±1.1	0.70±0.7	0.73±1.0	0.72±1.7
	SMDG (9,852)	0.73±1.5	0.64±1.1	0.72±1.4	0.64±0.9	<b>0.83±1.7</b>	0.67±1.1	0.64±1.2	0.67±1.3
	Pneumonia (20,412)	0.78±1.6	0.76±1.3	0.78±0.9	0.79±1.5	<b>0.81±1.7</b>	0.79±1.1	0.78±1.1	0.78±1.2
	<b>Average F1 Score</b>	0.77	0.71	0.77	0.76	<b>0.83</b>	0.77	0.76	0.76
<b>Combined Average Rank</b>		4.1	6.7	4.5	4.5	<b>2.4</b>	3.1	6.0	4.7

Table 3. Results with different ViT encoders (base/ large/ huge). Dataset size and parameter count are indicated in brackets. The best result for each dataset is highlighted, and the average rank for each fine-tuning method is shown at the end.

PEFT	Full FT (85.9M)	Attention (26.7M)	Bias (343K)	Norm (200K)	Bias+Norm (443K)	Bias+Norm+Attention (26.7M)	LoRA (SD) (797K)	SV-Diff (21.4K)
FID @ 2262 (10%)	7.15±1.1	8.35±1.3	22.43±0.9	20.25±1.2	31.26±1.1	<b>6.95±0.8</b>	11.84±0.7	14.80±0.8
FID @ 226 (1%)	10.43±0.9	8.44±0.7	32.90±1.3	29.67±1.2	36.76±0.7	<b>8.28±0.9</b>	14.88±1.3	16.48±1.4
Average FID	8.79	8.39	27.66	24.96	34.01	<b>7.61</b>	13.18	15.64
Combined Average Rank	2.5	2.5	7	6	8	<b>1</b>	5	5

Table 4. Comparing different strategies for fine-tuning the U-Net subcomponent of the stable diffusion pipeline text-to-image generation of chest x-rays. Fine-tuning Bias, Normalization, and Attention layers together (Bias+Norm+Attention) result in better performance (lower FID score) across both data volumes.

- Aaron Loh, Po-Hsuan Cameron Chen, Yuan Liu, Pinal Bavishi, Scott Mayer McKinney, Jim Winkens, Abhijit Guha Roy, Zach Beaver, Fiona Ryan, Justin Krogue, Mozziyar Etemadi, Umesh Telang, Yun Liu, Lily Peng, Greg S. Corrado, Dale R. Webster, David Fleet, Geoffrey Hinton, Neil Houlsby, Alan Karthikesalingam, Mohammad Norouzi, and Vivek Natarajan. Robust and efficient medical imaging with self-supervision, 2022. **1**
- [4] Shekoofeh Azizi, Basil Mustafa, Fiona Ryan, Zachary Beaver, Jan Freyberg, Jonathan Deaton, Aaron Loh, Alan Karthikesalingam, Simon Kornblith, Ting Chen, Vivek Natarajan, and Mohammad Norouzi. Big self-supervised models advance medical image classification. In *ICCV*, 2021. **1**
- [5] Yogesh Balaji, Seungjun Nah, Xun Huang, Arash Vahdat, Jiaming Song, Karsten Kreis, Miika Aittala, Timo Aila, Samuli Laine, Bryan Catanzaro, et al. ediffi: Text-to-image diffusion models with an ensemble of expert denoisers. *arXiv preprint arXiv:2211.01324*, 2022. **2**
- [6] Samyadeep Basu, Daniela Massiceti, Shell Xu Hu, and Soheil Feizi. Strong baselines for parameter efficient few-shot fine-tuning. *arXiv preprint arXiv:2304.01917*, 2023. **2, 3**
- [7] Elad Ben Zaken, Yoav Goldberg, and Shauli Ravfogel. BitFit: Simple parameter-efficient fine-tuning for transformer-based masked language-models. In *Proceedings of the 60th Annual Meeting of the Association for Computational Linguistics (Volume 2: Short Papers)*, pages 1–9, Dublin, Ireland, May 2022. Association for Computational Linguistics. **2, 3**
- [8] Rishi Bommasani et al. On the opportunities and risks of foundation models. *arXiv:2108.07258*, 2021. **1**
- [9] Tom Brown, Benjamin Mann, Nick Ryder, Melanie Subbiah, Jared D Kaplan, Prafulla Dhariwal, Arvind Neelakantan, Pranav Shyam, Girish Sastry, Amanda Askell, et al. Language models are few-shot learners. *Advances in neural information processing systems*, 33:1877–1901, 2020. **2**
- [10] Han Cai, Chuang Gan, Ligeng Zhu, and Song Han. Tinyt: Reduce memory, not parameters for efficient on-device learning. In H. Larochelle, M. Ranzato, R. Hadsell, M.F. Balcan, and H. Lin, editors, *Advances in Neural Information Processing Systems*, volume 33, pages 11285–11297. Curran Associates, Inc., 2020. **2, 3**
- [11] Pierre Chambon, Christian Bluethgen, Jean-Benoit Delbrouck, Rogier Van der Sluijs, Małgorzata Połacin, Juan Manuel Zambrano Chaves, Tanishq Mathew Abraham, Shivanshu Purohit, Curtis P. Langlotz, and Akshay Chaudhari. Roentgen: Vision-language foundation model for chest x-ray generation, 2022. **1, 2**

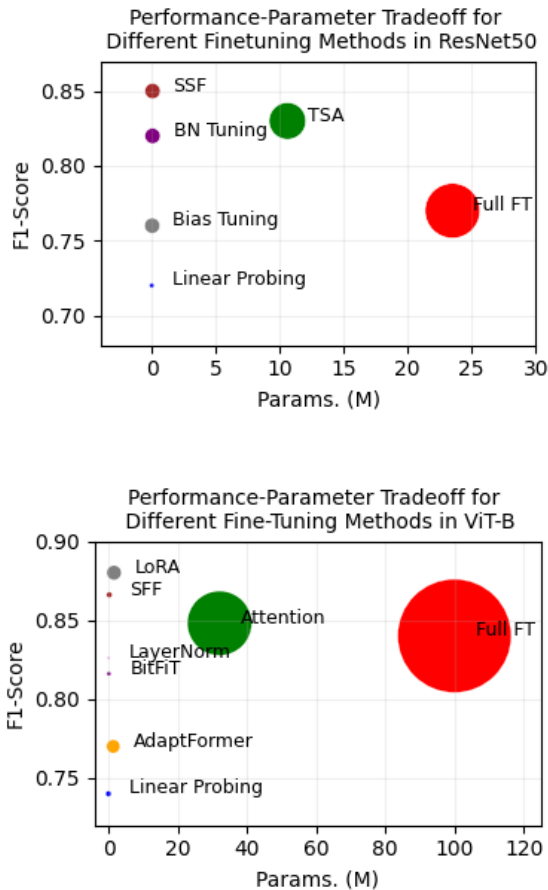


Figure 3. Performance v/s Parameter Count for ResNet50 and ViT-Base Encoders. The marker size indicates the tunable parameter count for each method.

- [12] Pierre Chambon, Christian Bluethgen, Curtis P Langlotz, and Akshay Chaudhari. Adapting pretrained vision-language foundational models to medical imaging domains. *arXiv preprint arXiv:2210.04133*, 2022. 6
- [13] Shoufa Chen, Chongjian Ge, Zhan Tong, Jiangliu Wang, Yibing Song, Jue Wang, and Ping Luo. Adaptformer: Adapting vision transformers for scalable visual recognition. *arXiv preprint arXiv:2205.13535*, 2022. 2, 3
- [14] Joseph Paul Cohen, Joseph D. Viviano, Paul Bertin, Paul Morrison, Parsa Torabian, Matteo Guarrera, Matthew P Lungren, Akshay Chaudhari, Rupert Brooks, Mohammad Hashir, and Hadrien Bertrand. TorchXRyVision: A library of chest X-ray datasets and models. In *Medical Imaging with Deep Learning*, 2022.
- [15] Jeffrey De Fauw, Joseph R Ledsam, Bernardino Romera-Paredes, Stanislav Nikolov, Nenad Tomasev, Sam Blackwell, Harry Askham, Xavier Glorot, Brendan O’Donoghue, Daniel Visentin, et al. Clinically applicable deep learning for diagnosis and referral in retinal disease. *Nature medicine*, 24(9):1342–1350, 2018. 1
- [16] Jia Deng, Wei Dong, Richard Socher, Li-Jia Li, Kai Li, and Li Fei-Fei. Imagenet: A large-scale hierarchical image database. In *2009 IEEE Conference on Computer Vision and Pattern Recognition*, pages 248–255, 2009. 5
- [17] Ruining Deng, Can Cui, Quan Liu, Tianyuan Yao, Lucas W Remedios, Shunxing Bao, Bennett A Landman, Lee E Wheless, Lori A Coburn, Keith T Wilson, et al. Segment anything model (sam) for digital pathology: Assess zero-shot segmentation on whole slide imaging. *arXiv preprint arXiv:2304.04155*, 2023. 3
- [18] Prafulla Dhariwal and Alexander Nichol. Diffusion models beat gans on image synthesis. *Advances in Neural Information Processing Systems*, 34:8780–8794, 2021. 2
- [19] Alexey Dosovitskiy, Lucas Beyer, Alexander Kolesnikov, Dirk Weissenborn, Xiaohua Zhai, Thomas Unterthiner, Mostafa Dehghani, Matthias Minderer, Georg Heigold, Sylvain Gelly, Jakob Uszkoreit, and Neil Houlsby. An image is worth 16x16 words: Transformers for image recognition at scale. In *International Conference on Learning Representations*, 2021. 1, 2, 5
- [20] Raman Dutt, Dylan Mendonca, Huai Ming Phen, Samuel Broida, Marzyeh Ghassemi, Judy Gichoya, Imon Banerjee, Tim Yoon, and Hari Trivedi. Automatic localization and brand detection of cervical spine hardware on radiographs using weakly supervised machine learning. *Radiology: Artificial Intelligence*, 4(2):e210099, 2022. 1
- [21] Andre Esteva, Brett Kuprel, Roberto A Novoa, Justin Ko, Susan M Swetter, Helen M Blau, and Sebastian Thrun. Dermatologist-level classification of skin cancer with deep neural networks. *nature*, 542(7639):115–118, 2017. 1
- [22] WA Falcon. Pytorch lightning, 2019.
- [23] Marc Fischer, Alexander Bartler, and Bin Yang. Prompt tuning for parameter-efficient medical image segmentation. *arXiv preprint arXiv:2211.09233*, 2022. 3
- [24] Jonathan Frankle, David J. Schwab, and Ari S. Morcos. Training batchnorm and only batchnorm: On the expressive power of random features in cnns. *CoRR*, abs/2003.00152, 2020. 2, 3
- [25] Henry Gouk, Timothy Hospedales, et al. Distance-based regularisation of deep networks for fine-tuning. In *International Conference on Learning Representations*, 2020. 1
- [26] Matthew Groh, Caleb Harris, Roxana Daneshjou, Omar Badri, and Arash Koochek. Towards transparency in dermatology image datasets with skin tone annotations by experts, crowds, and an algorithm. *arXiv preprint arXiv:2207.02942*, 2022. 5
- [27] Matthew Groh, Caleb Harris, Luis Soenksen, Felix Lau, Rachel Han, Aerin Kim, Arash Koochek, and Omar Badri. Evaluating deep neural networks trained on clinical images in dermatology with the fitzpatrick 17k dataset. In *Proceedings of the IEEE/CVF Conference on Computer Vision and Pattern Recognition*, pages 1820–1828, 2021. 5
- [28] Ligong Han, Yinxiao Li, Han Zhang, Peyman Milanfar, Dimitris Metaxas, and Feng Yang. Svdiff: Compact parameter space for diffusion fine-tuning. *arXiv preprint arXiv:2303.11305*, 2023. 3
- [29] Junxian He, Chunting Zhou, Xuezhe Ma, Taylor Berg-Kirkpatrick, and Graham Neubig. Towards a unified view of parameter-efficient transfer learning. In *International Conference on Learning Representations*, 2022. 1
- [30] Kaiming He, Xiangyu Zhang, Shaoqing Ren, and Jian Sun. Deep residual learning for image recognition. In *Proceedings of the IEEE conference on computer vision and pattern recognition*, pages 770–778, 2016. 5
- [31] Jonathan Ho, Ajay Jain, and Pieter Abbeel. Denoising diffusion probabilistic models. *Advances in Neural Information Processing Systems*, 33:6840–6851, 2020. 2

- [32] Arthur S Hong, David Levin, Laurence Parker, Vijay M Rao, Dennis Ross-Degnan, and J Frank Wharam. Trends in diagnostic imaging utilization among medicare and commercially insured adults from 2003 through 2016. *Radiology*, 294(2):342–350, 2020. 1
- [33] Neil Houlsby, Andrei Giurgiu, Stanislaw Jastrzebski, Bruna Morroni, Quentin De Laroussilhe, Andrea Gesmundo, Mona Attariyan, and Sylvain Gelly. Parameter-efficient transfer learning for nlp. In *International Conference on Machine Learning*, pages 2790–2799. PMLR, 2019. 2, 3
- [34] Edward J Hu, yelong shen, Phillip Wallis, Zeyuan Allen-Zhu, Yuanzhi Li, Shean Wang, Lu Wang, and Weizhu Chen. LoRA: Low-rank adaptation of large language models. In *International Conference on Learning Representations*, 2022. 1, 2, 3
- [35] Gao Huang, Zhuang Liu, Laurens Van Der Maaten, and Kilian Q Weinberger. Densely connected convolutional networks. In *Proceedings of the IEEE conference on computer vision and pattern recognition*, pages 4700–4708, 2017.
- [36] Shih-Cheng Huang, Anuj Pareek, Malte Jensen, Matthew P Lungren, Serena Yeung, and Akshay S. Chaudhari. Self-supervised learning for medical image classification: a systematic review and implementation guidelines. 1
- [37] Menglin Jia, Luming Tang, Bor-Chun Chen, Claire Cardie, Serge Belongie, Bharath Hariharan, and Ser-Nam Lim. Visual prompt tuning. In *Computer Vision – ECCV 2022: 17th European Conference, Tel Aviv, Israel, October 23–27, 2022, Proceedings, Part XXXIII*, page 709–727, Berlin, Heidelberg, 2022. Springer-Verlag. 2
- [38] Alistair EW Johnson, Tom J Pollard, Nathaniel R Greenbaum, Matthew P Lungren, Chih-ying Deng, Yifan Peng, Zhiyong Lu, Roger G Mark, Seth J Berkowitz, and Steven Horng. Mimic-cxr-jpg, a large publicly available database of labeled chest radiographs. *arXiv preprint arXiv:1901.07042*, 2019. 6
- [39] Sergey Kastruyulin, Dzhamil Zakirov, and Denis Prokopenko. PyTorch Image Quality: Metrics and measure for image quality assessment, 2019. Open-source software available at <https://github.com/photosynthesis-team/piq>.
- [40] Sergey Kastruyulin, Jamil Zakirov, Denis Prokopenko, and Dmitry V. Dylov. Pytorch image quality: Metrics for image quality assessment, 2022.
- [41] Diederik Kingma, Tim Salimans, Ben Poole, and Jonathan Ho. Variational diffusion models. *Advances in neural information processing systems*, 34:21696–21707, 2021. 2
- [42] Alexander Kirillov, Eric Mintun, Nikhila Ravi, Hanzi Mao, Chloe Rolland, Laura Gustafson, Tete Xiao, Spencer Whitehead, Alexander C Berg, Wan-Yen Lo, et al. Segment anything. *arXiv preprint arXiv:2304.02643*, 2023. 2, 3
- [43] Brian Lester, Rami Al-Rfou, and Noah Constant. The power of scale for parameter-efficient prompt tuning. *arXiv preprint arXiv:2104.08691*, 2021. 2
- [44] Lisha Li, Kevin Jamieson, Afshin Rostamizadeh, Katya Gonina, Moritz Hardt, Benjamin Recht, and Ameet Talwalkar. Massively parallel hyperparameter tuning, 2018. 5
- [45] Wei-Hong Li, Xialei Liu, and Hakan Bilen. Cross-domain few-shot learning with task-specific adapters. In *Proceedings of the IEEE/CVF Conference on Computer Vision and Pattern Recognition*, pages 7161–7170, 2022. 2, 3, 4
- [46] Xiang Lisa Li and Percy Liang. Prefix-tuning: Optimizing continuous prompts for generation. *arXiv preprint arXiv:2101.00190*, 2021. 2
- [47] Dongze Lian, Daquan Zhou, Jiashi Feng, and Xinchao Wang. Scaling & shifting your features: A new baseline for efficient model tuning. *arXiv preprint arXiv:2210.08823*, 2022. 2, 3
- [48] Richard Liaw, Eric Liang, Robert Nishihara, Philipp Moritz, Joseph E Gonzalez, and Ion Stoica. Tune: A research platform for distributed model selection and training. *arXiv preprint arXiv:1807.05118*, 2018.
- [49] Veena Mayya, Sowmya Kamath S., and Uma Kulkarni. Automated microaneurysms detection for early diagnosis of diabetic retinopathy: A comprehensive review. *Computer Methods and Programs in Biomedicine Update*, 1:100013, 2021
- [50] Scott Mayer McKinney, Marcin Sieniek, Varun Godbole, Jonathan Godwin, Natasha Antropova, Hutun Ashrafian, Trevor Back, Mary Chesus, Greg S Corrado, Ara Darzi, et al. International evaluation of an ai system for breast cancer screening. *Nature*, 577(7788):89–94, 2020. 1
- [51] Taehong Moon, Moonseok Choi, Gayoung Lee, Jung-Woo Ha, and Juho Lee. Fine-tuning diffusion models with limited data. In *NeurIPS 2022 Workshop on Score-Based Methods*. 3
- [52] Radiological Society of North America. Rsn pneumonia detection dataset. Available at: <https://www.kaggle.com/competitions/rsna-pneumonia-detection-challenge/data>, 2018. Accessed: October, 2022. 5
- [53] Adam Paszke, Sam Gross, Francisco Massa, Adam Lerer, James Bradbury, Gregory Chanan, Trevor Killeen, Zeming Lin, Natalia Gimelshein, Luca Antiga, et al. Pytorch: An imperative style, high-performance deep learning library. *Advances in neural information processing systems*, 32, 2019.
- [54] William Peebles and Saining Xie. Scalable diffusion models with transformers. *arXiv preprint arXiv:2212.09748*, 2022. 2
- [55] Yujia Qin, Xiaozhi Wang, Yusheng Su, Yankai Lin, Ning Ding, Jing Yi, Weize Chen, Zhiyuan Liu, Juanzi Li, Lei Hou, Peng Li, Maosong Sun, and Jie Zhou. Exploring universal intrinsic task subspace via prompt tuning. 2021. 2
- [56] Alec Radford, Jong Wook Kim, Chris Hallacy, Aditya Ramesh, Gabriel Goh, Sandhini Agarwal, Girish Sastry, Amanda Askell, Pamela Mishkin, Jack Clark, et al. Learning transferable visual models from natural language supervision. In *International conference on machine learning*, pages 8748–8763. PMLR, 2021.
- [57] Sylvestre-Alvise Rebuffi, Hakan Bilen, and Andrea Vedaldi. Learning multiple visual domains with residual adapters. *Advances in neural information processing systems*, 30, 2017. 2
- [58] Sylvestre-Alvise Rebuffi, Hakan Bilen, and Andrea Vedaldi. Efficient parametrization of multi-domain deep neural networks. In *Proceedings of the IEEE Conference on Computer Vision and Pattern Recognition*, pages 8119–8127, 2018. 1, 2
- [59] Tal Ridnik, Emanuel Ben-Baruch, Asaf Noy, and Lihi Zelnik. Imagenet-21k pretraining for the masses. In J. Vanschoren and S. Yeung, editors, *Proceedings of the Neural Information Processing Systems Track on Datasets and Benchmarks*, volume 1. Curran, 2021. 5
- [60] Robin Rombach, Andreas Blattmann, Dominik Lorenz, Patrick Esser, and Björn Ommer. High-resolution image synthesis with latent diffusion models. In *Proceedings of the IEEE/CVF*

- Conference on Computer Vision and Pattern Recognition*, pages 10684–10695, 2022. 2
- [61] Olaf Ronneberger, Philipp Fischer, and Thomas Brox. U-net: Convolutional networks for biomedical image segmentation. In Nassir Navab, Joachim Hornegger, William M. Wells, and Alejandro F. Frangi, editors, *Medical Image Computing and Computer-Assisted Intervention – MICCAI 2015*, pages 234–241, Cham, 2015. Springer International Publishing. 3
- [62] Chitwan Saharia, William Chan, Saurabh Saxena, Lala Li, Jay Whang, Emily L Denton, Kamyar Ghasemipour, Raphael Gontijo Lopes, Burcu Karagol Ayan, Tim Salimans, et al. Photorealistic text-to-image diffusion models with deep language understanding. *Advances in Neural Information Processing Systems*, 35:36479–36494, 2022. 2
- [63] Timo Schick and Hinrich Schütze. It’s not just size that matters: Small language models are also few-shot learners. *arXiv preprint arXiv:2009.07118*, 2020. 2
- [64] Julio Silva-Rodríguez, Jose Dolz, and Ismail Ben Ayed. Transductive few-shot adapters for medical image segmentation. *arXiv preprint arXiv:2303.17051*, 2023. 3
- [65] Lysandre Debut Younes Belkada Sayak Paul Sourab Mangrulkar, Sylvain Gugger. Peft: State-of-the-art parameter-efficient fine-tuning methods. <https://github.com/huggingface/peft>, 2022.
- [66] Hugo Touvron, Matthieu Cord, Alaaeldin El-Nouby, Jakob Verbeek, and Hervé Jégou. Three things everyone should know about vision transformers. In *Computer Vision–ECCV 2022: 17th European Conference, Tel Aviv, Israel, October 23–27, 2022, Proceedings, Part XXIV*, pages 497–515. Springer, 2022. 2, 3
- [67] Philipp Tschandl. The HAM10000 dataset, a large collection of multi-source dermatoscopic images of common pigmented skin lesions, 2018. 4, 5
- [68] Patrick von Platen, Suraj Patil, Anton Lozhkov, Pedro Cuenca, Nathan Lambert, Kashif Rasul, Mishig Davaadorj, and Thomas Wolf. Diffusers: State-of-the-art diffusion models. <https://github.com/huggingface/diffusers>, 2022.
- [69] Ross Wightman. Pytorch image models. <https://github.com/rwightman/pytorch-image-models>, 2019.
- [70] Martin J Willeminck, Wojciech A Koszek, Cailin Hardell, Jie Wu, Dominik Fleischmann, Hugh Harvey, Les R Folio, Ronald M Summers, Daniel L Rubin, and Matthew P Lungren. Preparing medical imaging data for machine learning. *Radiology*, 295(1):4–15, 2020. 1
- [71] Junde Wu, Rao Fu, Huihui Fang, Yuanpei Liu, Zhaowei Wang, Yanwu Xu, Yueming Jin, and Tal Arbel. Medical sam adapter: Adapting segment anything model for medical image segmentation. *arXiv preprint arXiv:2304.12620*, 2023. 3
- [72] Chendong Xiang, Fan Bao, Chongxuan Li, Hang Su, and Jun Zhu. A closer look at parameter-efficient tuning in diffusion models. *arXiv preprint arXiv:2303.18181*, 2023. 3
- [73] Enze Xie, Lewei Yao, Han Shi, Zhili Liu, Daquan Zhou, Zhaoqiang Liu, Jiawei Li, and Zhenguo Li. DiffFit: Unlocking transferability of large diffusion models via simple parameter-efficient fine-tuning. *arXiv preprint arXiv:2304.06648*, 2023. 1, 2
- [74] LI Xuhong, Yves Grandvalet, and Franck Davoine. Explicit inductive bias for transfer learning with convolutional networks. In *International Conference on Machine Learning*, pages 2825–2834. PMLR, 2018. 1
- [75] Fabian SL Yii, Raman Dutt, Tom MacGillivray, Baljean Dhillon, Miguel Bernabeu, and Niall Strang. Rethinking retinal image quality: Treating quality threshold as a tunable hyperparameter. In *Ophthalmic Medical Image Analysis: 9th International Workshop, OMIA 2022, Held in Conjunction with MICCAI 2022, Singapore, Singapore, September 22, 2022, Proceedings*, pages 73–83. Springer, 2022. 1
- [76] Kaidong Zhang and Dong Liu. Customized segment anything model for medical image segmentation. *arXiv preprint arXiv:2304.13785*, 2023. 3
- [77] S Kevin Zhou, Hayit Greenspan, Christos Davatzikos, James S Duncan, Bram Van Ginneken, Anant Madabhushi, Jerry L Prince, Daniel Rueckert, and Ronald M Summers. A review of deep learning in medical imaging: Imaging traits, technology trends, case studies with progress highlights, and future promises. *Proceedings of the IEEE*, 109(5):820–838, 2021. 1